Composite Analyses of Low-Skill Arctic Cyclones During Summer

Kevin A. Biernat*, Daniel Keyser, and Lance F. Bosart

*E-mail: kbiernat@albany.edu

University at Albany, SUNY
Department of Atmospheric and Environmental Sciences

Presented at 101st AMS Annual Meeting on 14 January 2021

Poster number: 747

This research is supported by Office of Naval Research Grant N00014-18-1-2200

1) Background

- Arctic cyclones (ACs) are synoptic-scale low pressure systems that frequently form over the Arctic or move into the Arctic from Eurasia during summer (e.g., Crawford and Serreze 2016).
- Interactions between ACs and the synoptic-scale flow over the Arctic, baroclinic processes, and latent heating may influence the evolution of ACs and the synoptic-scale flow over the Arctic (e.g., Tao et al. 2017; Yamagami et al. 2017).
- It is anticipated that relatively low forecast skill of ACs and the synoptic-scale flow over the Arctic may be attributed in part to forecast error growth accompanying interactions between ACs and the synoptic-scale flow over the Arctic, baroclinic processes, and latent heating.
- The purpose of this study is to examine dynamical and thermodynamic quantities characterizing the Arctic environment and low-skill ACs during periods of low and high forecast skill of the synoptic-scale flow over the Arctic.

2) Data and methods

Evaluation of Arctic forecast skill

- Utilize day-5 forecasts of 500-hPa geopotential height initialized at 0000 UTC during summers (June, July, and August) of 2007–2017 from 11-member GEFS reforecast dataset v2 (Hamill et al. 2013).
- Calculate standardized anomaly of area-averaged root mean square error (RMSE; ERA-Interim used as verification) of 500-hPa geopotential height over the Arctic (≥ 70°N) following Moore (2017).
- Refer to forecast days valid at day 5 associated with the top and bottom 10% of aforementioned standardized anomaly as low-skill days and high-skill days, respectively.
- Refer to forecasts initialized five days prior to low-skill days and high-skill days as low-skill forecasts and high-skill forecasts, respectively.
- Refer to time periods through day 5 encompassed by low-skill forecasts and high-skill forecasts as low-skill periods and high-skill periods, respectively.

Identification of low-skill ACs

- Create a 2007–2017 summer AC climatology by obtaining cyclone tracks from 1° ERA-Interim (Dee et al. 2011) cyclone climatology prepared by Sprenger et al. (2017), and requiring cyclones to last ≥ 2 days and spend at least some portion of their lifetimes in the Arctic (> 70°N).
- Track ACs in forecasts from GEFS reforecast dataset v2 initialized 120 h prior to time of lowest sea level pressure (SLP) of ACs when located in the Arctic during low-skill periods and high-skill periods using an objective cyclone tracking algorithm (Crawford et al. 2020).
- Calculate 120-h intensity RMSE (ERA-Interim used as verification) based on minimum SLP of ACs at aforementioned time of lowest SLP, and refer to ACs associated with the top 25% of 120-h intensity RMSE for low-skill periods and high-skill periods as low-skill ACs for these respective periods.

6) Discussion

- There tends to be statistically significantly amplified synoptic-scale flow (Fig. 1a), and statistically significantly high values of lower-to-midtropospheric Eady growth rate (Fig. 1b), IVT (Fig. 1c), lower-to-midtropospheric ascent (Fig. 1d), and upper-tropospheric divergence (Fig. 1e) over the Arctic during low-skill periods, with opposite results during high-skill periods.
- Low-skill ACs during low-skill periods tend to be stronger (Fig. 2a), and embedded within a region of more amplified synoptic-scale flow (Fig. 2b), higher values of lower-to-midtropospheric Eady growth rate (Fig. 2c), higher values of IVT (Fig. 2d), higher values of lower-to-midtropospheric ascent (Fig. 2e), higher values of upper-tropospheric divergence (Fig. 2f), and lower forecast skill of the synoptic-scale flow (Fig. 2g) compared to low-skill ACs during high-skill periods.
- Statistically significantly high values of IVT (Fig. 2d), lower-to-midtropospheric ascent (Fig. 2e), and upper-tropospheric divergence (Fig. 2f) surrounding low-skill ACs during low-skill periods suggest that there may be anomalously high values of latent heating surrounding these ACs.
- The aforementioned latent heating and statistically significantly high values of lower-to-midtropospheric Eady growth rate surrounding low-skill ACs during low-skill periods (Fig. 2c) likely contribute to these ACs being statistically significantly strong (Fig. 2a).
- Forecast error growth that may accompany 1) the interaction of low-skill ACs during low-skill periods with the synoptic-scale flow, 2) baroclinic processes (related to Eady growth rate), and 3) latent heating may contribute to the low forecast skill of these ACs and to the statistically significantly low forecast skill of the synoptic-scale flow surrounding these ACs (Fig. 2g).
- An example low-skill AC during a low-skill period intensifies in a region of strong baroclinicity (Fig. 3a) downstream of a midtropospheric vorticity maximum (Fig. 3b) as the AC interacts with moderately amplified synoptic-scale flow (Fig. 3c; Table 1).
- Relatively high lower-to-midtropospheric Eady growth rates associated with the strong baroclinicity (Fig. 3d; Table 1), midtropospheric forcing for ascent (suggested by Fig. 3b), upper-tropospheric jet coupling (Fig. 3a), and relatively high values of IVT (Fig. 3e; Table 1) likely support the relatively high values of lower-to-midtropospheric ascent and upper-tropospheric divergence in the vicinity of the example low-skill AC (Fig. 3f; Table 1) and the concomitant intensification of the AC.
- The most extreme values of the quantities for the example low-skill AC given in Table 1 are high with respect to the corresponding distributions for low-skill ACs during low-skill periods given in Fig. 2.

3) Quantities characterizing the Arctic environment

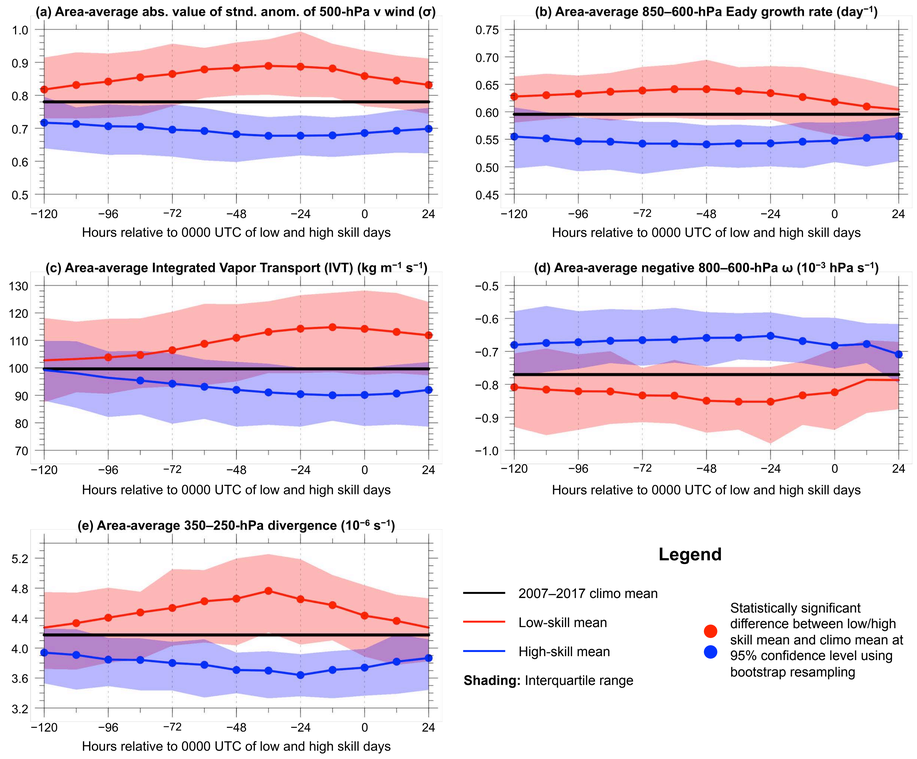

FIG. 1. Distribution of selected quantities area-averaged over the Arctic (≥ 70°N) during low-skill periods (red), high-skill periods (blue), and the 2007–2017 climatology (black). There are 101 low-skill days and 101 high-skill days. Data source: ERA-Interim.

4) Quantities characterizing low-skill ACs

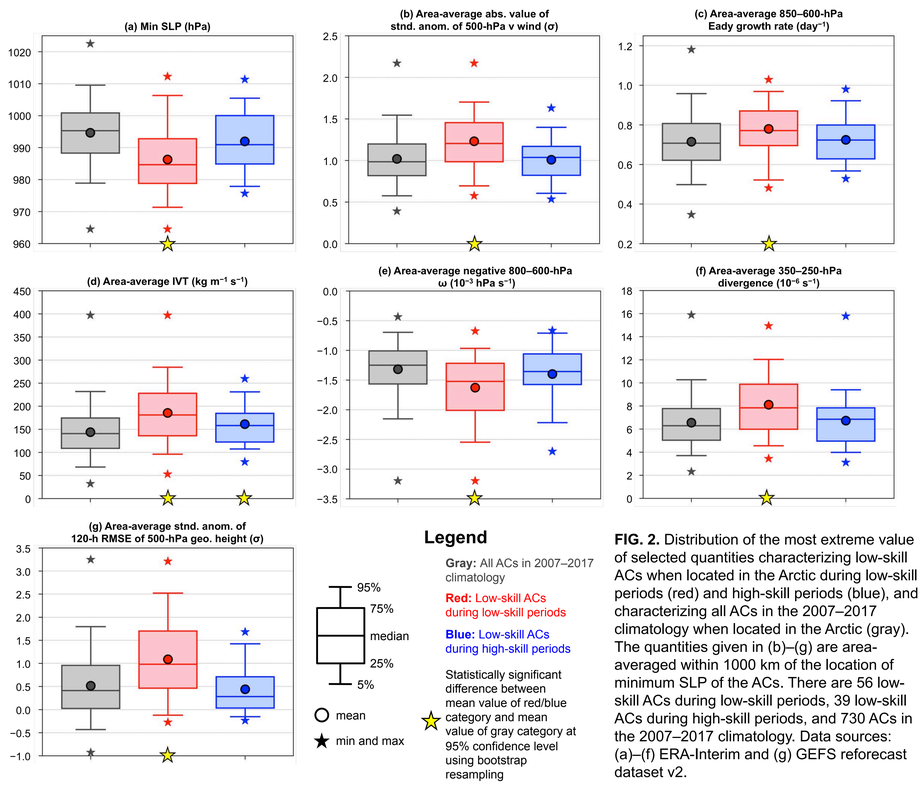

FIG. 2. Distribution of the most extreme value of selected quantities characterizing low-skill ACs when located in the Arctic during low-skill periods (red) and high-skill periods (blue), and characterizing all ACs in the 2007–2017 climatology when located in the Arctic (gray). The quantities given in (b)–(g) are area-averaged within 1000 km of the location of minimum SLP of the ACs. There are 56 low-skill ACs during low-skill periods, 39 low-skill ACs during high-skill periods, and 730 ACs in the 2007–2017 climatology. Data sources: (a)–(f) ERA-Interim and (g) GEFS reforecast dataset v2.

5) Example low-skill AC during a low-skill period

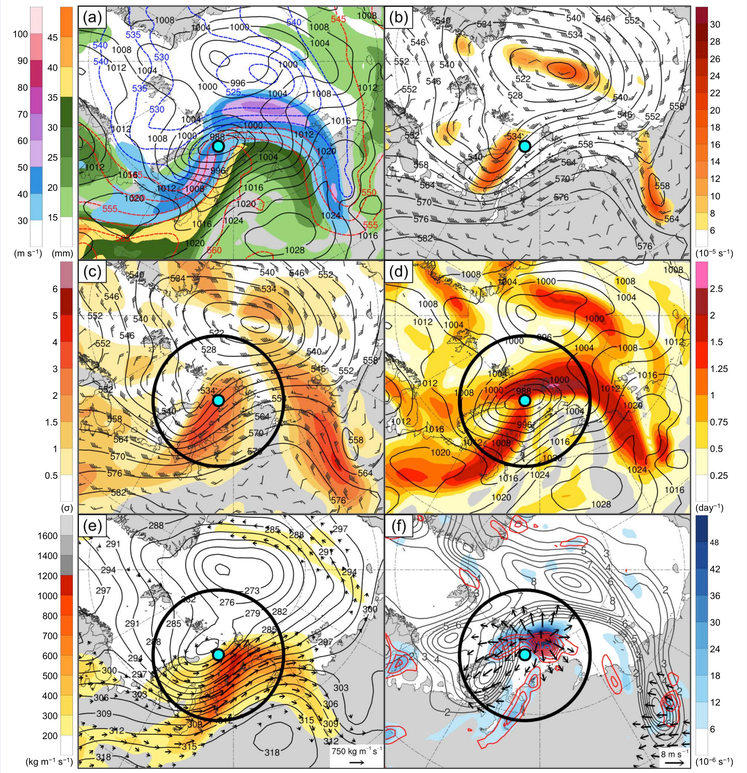

FIG. 3. ERA-Interim analyses valid at 0000 UTC 14 Aug 2016. The cyan dot shows the location of an example low-skill AC occurring at the aforementioned time during a low-skill period, and the 1000-km radius black circle surrounding the location of the AC shows where the area-averaged quantities given in Table 1 are calculated.

(a) 300-hPa wind speed (m s^{-1}, shaded), precipitable water (mm, shaded), 1000–500-hPa thickness (dam, dashed red and blue), and SLP (hPa, black).

(b) 500-hPa relative vorticity (10^{-5} s^{-1}, shaded), geopotential height (dam, black), and wind (m s^{-1}, flags and barbs).

(c) Absolute value of standardized anomaly of 500-hPa v wind (σ, shaded), and 500-hPa geopotential height (dam, black) and wind (m s^{-1}, flags and barbs).

(d) 850–600-hPa Eady growth rate (day^{-1}, shaded) and SLP (hPa, black).

(e) IVT (kg m^{-1} s^{-1}, shaded and vectors) and 700-hPa geopotential height (dam, black).

(f) Negative 800–600-hPa ω (red contours every 2 x 10^{-3} hPa s^{-1}), and 350–250-hPa divergence (10^{-6} s^{-1}, shaded), irrotational wind (m s^{-1}, vectors), and potential vorticity (PVU, gray).

Table 1. Same quantities as in Fig. 2 characterizing the example low-skill AC. The value of these quantities at 0000 UTC 14 Aug 2016 and the most extreme value of these quantities when the AC is located in the Arctic during the low-skill period are given. The area-averaged quantities are calculated within 1000 km of the location of minimum SLP of the AC (within the black circle shown in Figs. 3c–f for 0000 UTC 14 Aug 2016).

	Value at 0000 UTC 14 Aug 2016	Most extreme value (compare to red category in Fig. 2)
Min SLP (hPa)	984.4	967.3
Area-average abs. value of stnd. anom. of 500-hPa v wind (σ)	1.01	1.60
Area-average 850–600-hPa Eady growth rate (day^{-1})	0.85	0.92
Area-average IVT (kg m^{-1} s^{-1})	314.0	323.0
Area-average negative 800–600-hPa ω (10^{-3} hPa s^{-1})	−2.41	−2.58
Area-average 350–250-hPa divergence (10^{-6} s^{-1})	12.0	12.0
Area-average stnd. anom. of 120-h RMSE of 500-hPa geo. height (σ)	0.79	1.86

References

- Crawford, A. D., and M. C. Serreze, 2016: Does the summer Arctic frontal zone influence Arctic Ocean cyclone activity? *J. Climate*, **29**, 4977–4993.
- Crawford, A. D., K. E. Alley, A. M. Cooke, and M. C. Serreze, 2020: Synoptic Climatology of rain-on-snow events in Alaska. *Mon. Wea. Rev.*, **148**, 1275–1295.
- Dee, D. P., and Coauthors, 2011: The ERA-Interim reanalysis: Configuration and performance of the data assimilation system. *Quart. J. Roy. Meteor. Soc.*, **137**, 553–597.
- Hamill, T. M., G. T. Bates, J. S. Whitaker, D. R. Murray, M. Fiorino, T. J. Galarneau Jr., Y. Zhu, and W. Lapenta, 2013: NOAA's second-generation global medium-range ensemble reforecast dataset. *Bull. Amer. Meteor. Soc.*, **94**, 1553–1565.
- Moore, B. J., 2017: Rossby wave breaking and widespread extreme precipitation events in the central and eastern U.S. Ph.D. dissertation, University at Albany, State University of New York, Albany, NY, 182 pp.
- Sprenger, M., and Coauthors, 2017: Global climatologies of Eulerian and Lagrangian flow features based on ERA-Interim. *Bull. Amer. Meteor. Soc.*, **98**, 1739–1748.
- Tao, W., J. Zhang, Y. Fu, and X. Zhang, 2017: Driving roles of tropospheric and stratospheric thermal anomalies in intensification and persistence of the Arctic superstorm in 2012. *Geophys. Res. Lett.*, **44**, 10017–10025.
- Yamagami, A., M. Matsueda, and H. L. Tanaka, 2017: Extreme Arctic cyclone in August 2016. *Atmos. Sci. Lett.*, **18**, 307–314.